Hydrogen-Assisted Fatigue Crack Growth Model for Type 304 Stainless Steel in Simulated BWR Environments

Zuhair M. Gasem[1,2]

[1]Mechanical Engineering Department, College of Engineering and Physics, King Fahd University of Petroleum and Minerals, Dhahran, 31261, Saudi Arabia.
[2]Interdisciplinary Research Center for Advanced Materials, King Fahd University of Petroleum & Minerals, Dhahran, 31261, Saudi Arabia. Email: zuhair@kfupm.edu.sa

Abstract – The current design and evaluation codes for life assessment of critical parts exposed to the harsh environment of light water reactors and susceptible to environmentally-assisted fatigue crack growth (EA-FCG) are commonly based on empirical data and often are highly conservative. Data from the open literature for fatigue crack growth rates (da/dN) vs. frequency for different metallurgical conditions of type 304 stainless steels (304 SS) in high-temperature water demonstrate that the crack advancement can be adequately described by da/dN $\propto 1/(f)^\alpha$ where α varies depending on the alloy microstructure, applied stress intensity factor range (ΔK), loading ratio (R), and water chemistry. Similar f-dependent FCG behaviors have been frequently reported for a variety of 304 SS in aqueous solutions and in pressurized hydrogen gas environments at ambient temperature. This paper aims to characterize the f-dependent EA-FCG of 304 SS in a boiling water reactor with hydrogen water chemistry (BWR/HWC) environment and to propose a mechanistic model where hydrogen-diffusion in the crack-tip process zone is the rate-limiting step for environmental accelerated cracking. The model assumes that the upper bound EA-FCG rate correlates with the crack-tip distance where the local tensile stress and hydrogen concentration are maximum. The model predicts an f-independent upper bound EA-FCG rate for 304 SS as a function of the maximum stress intensity factor (K_{max}) and the elevated temperature elastic modulus and yield stress. The model prediction shows good agreement with EA-FCG data for 304 SS tested at very low frequencies in BWR/HWC environments with lower margins of error as compared to the existing assessment reference curves.

Keywords: Environmentally-assisted fatigue crack growth, frequency effect, hydrogen diffusion, solution annealed 304 stainless steel, hydrogen embrittlement

I. Introduction

Renewal of the operational license of light water reactors (LWR) beyond the design life of 40 to 60-80 years requires systematic implementation of life-assessment analyses and evaluation techniques especially for critical parts that are susceptible to environmentally-assisted cracking. Extensive experimental work based on linear elastic fracture mechanics (LEFM) under simulated primary-circuit pressurized water reactor (PWR) and boiling water reactor (BWR) conditions have shown that austenitic stainless steels (ASS) are susceptible to environmentally-assisted fatigue crack growth (EA-FCG) relative to comparable tests in dry air at the same temperature [1], [2]. The degree of environmental enhancement has been found to strongly depend on the applied stress intensity factor range (ΔK), stress ratio (R), loading frequency, and temperature [3]. No significant effects have been observed on FCG in LWR environments for different heat treatments (solution annealed, sensitized, or stabilized), the carbon content (304 vs. 304L), steel grade (304L vs. 316L), grain size, yield strength, and specimen orientation [3].

For evaluation of fatigue cracks in nuclear power plant components, the American Society of Mechanical Engineers (ASME) Boiler and Pressure Vessel Code Section XI provides a reference FCG curve for ASS in dry air environments as a function of temperature, ΔK, and R:

$$da/dN_{air} = C_o\, S(R)\, \Delta K^{3.3} \quad (1)$$

where,

$$\log(C_o) = -8.714 + 1.34 \times 10^{-3}\, T - 3.34 \times 10^{-6}\, T^2 + 5.95 \times 10^{-9}\, T^3$$

$$S\,(R) = \begin{cases} 1 + 1.8\,R & for\ R < 0.79 \\ -43.35 + 57.97\,R & for\ R > 0.79 \end{cases}$$

The Japanese Society of Mechanical Engineers (JSME) code proposed an FCG formula for normal water chemistry (NWC) in BWR condition incorporating the effect of the loading rise time (Δt_R). The formula predicts conservative rates for solution-annealed stabilized ASS grades [4]:

$$\boldsymbol{da/dN_{H_2O} = 8.17x10^{-12}\, \Delta t_R^{0.5}\, \frac{\Delta K^{3.3}}{(1-R)^{2.12}}}\ \boldsymbol{(2)}$$

where da/dN in m/cycle, Δt_R in s, and ΔK in MPa√m. Assuming a symmetrical waveform, Δt_R can be replaced by $1/(2{*}f)$ and Eq. (2) can be rewritten as:

$$da/dN_{H_2O} = 8.17x10^{-12}\, \frac{1}{\sqrt{2}f^{0.50}}\, \frac{\Delta K^{3.3}}{(1-R)^{2.12}}\ (3)$$

where f is the loading frequency (Hz).

Eq. (3) predicts a power law f-dependent FCG behavior with a slope of -0.5 for ASS in a BWR/NWC environment. In addition, the reference curve predicts that the EA-FCG rate for ASS in high-temperature water environments increased continuously with decreases in the loading frequency with no saturation of environmental effect predicted.

The above empirical reference curves are based on experimental FCG data conducted over a range of frequencies. A more accurate prediction can be obtained through mechanistic modeling based on understanding the crack-tip processes that contribute to the crack advancement. One approach to quantify the effect of the environment on the EA-FCG is to separate the mechanical (ΔK and R) and the chemical effects by conducting EA-FCG tests under constant ΔK and high R conditions (to avoid retardation related to crack closure) over a wider range of frequencies. This approach allows better characterization of the frequency-cycle (time per cycle) crack-tip governing process. This testing technique has been employed by numerous studies to examine the EA-FCG of a variety of alloy/environment combinations at ambient as well as at high water temperatures.

The objective of this paper is to investigate the f-dependent FCG data for a typical ASS such as 304 SS in BWR environments from the open literature and to propose a mechanistic model based on hydrogen diffusion as the rate-limiting step in the crack-tip process zone for high-temperature water.

II. F-dependent FCG Data in LWRs

Seifert et al. [3] reported f-dependent EA-FCP data under constant ΔK loading for sensitized and solution-annealed (SA) 304 SS under BWR/NWC and for SA 304L SS under BWR hydrogenated water chemistry (HWC) conditions. The EA-FCP rates increased with decreases in the loading frequency and followed a power law for f < 0.1 Hz:

$$da/dN_{H_2O} = B/f^n \quad (4)$$

where B is a constant that depended on the mechanical loading parameters (ΔK and R) while the exponent n was found to vary depending on the testing conditions. Figure 1 presents f-dependent FCG data for different metallurgical conditions of 304 SS in BWR/NWC and BWR/HWC showing the general trend of Eq. (4) as reported by Seifert et al. [3]. Table 1 summarizes the data reported with the regression values of n for each material/environment condition.
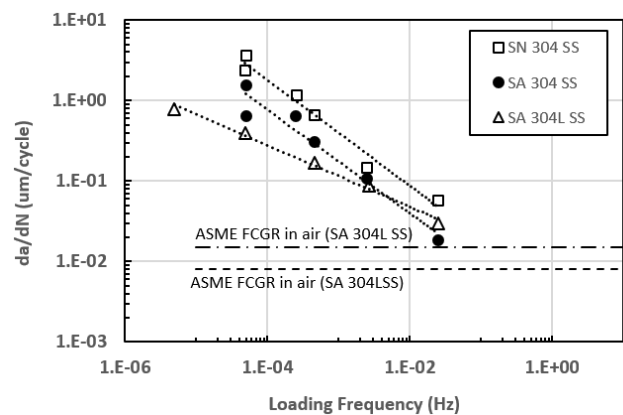

Fig. 1. FCG rate vs. loading frequency for SA 304 SS and SN 304 SS under BWR/NWC and SA 304L SS under BWR/HWC condition. Data reproduced from [3].

Table 1 Regression analysis of power-law frequency dependent FCP data in different BWR conditions based on Eq. (4). SA 304 (solution annealed); SN 304 (sensitized).

Material	ΔK (MPa√m)	R	Environment	n
SA 304 SS	7.1-8.4 (K_{max}=30.0)	0.742	NWC (400 ppb O_2, T= 288°C)	0.66
SN 304 SS	7.1-8.4 (K_{max}=30.0)	0.742	=	0.66
SA 304L SS	10.9-11.3 (K_{max}=22.0)	0.50	HWC (150 ppb H_2, T=200°C)	0.38

III. F-Dependent FCG Data at RT

Several past studies have investigated the EA-FCG of type 304 SS tested at constant ΔK in different aqueous chloride solutions at room temperature over a wide frequency range of 30～0.1 Hz [5], [6], [7], [8], [9]. The results typically revealed that the intrinsic EA-FCG rates of 304 SS at constant ΔK in different 3.5% NaCl solutions generally showed a single frequency-dependent regime where da/dN increased as the frequency was reduced, similar to the response shown in Fig. 1 for high-temperature water. However, these studies lacked EA-FCG data at frequencies below 0.1 Hz to characterize the full spectrum effect of f-dependent EA-FCG. This is primarily due to the time-consuming nature of FCG tests at very low frequencies.

A more recent study has investigated the f-dependent hydrogen-assisted fatigue crack growth (HA-FCG) response of SA 304 SS under constant ΔK condition and a fixed loading ratio of 0.1 in high purity hydrogen gas environment for a wider range of frequencies (5～0.001 Hz) [10], [11], [12]. The authors examined the effect of H_2 as an external environment using non-pre-charged specimens and tested hydrogen pre-charged specimens both in 0.7 MPa H_2 gas chamber to investigate the effect of external and internal hydrogen on the f-dependent FCG behavior of 304 SS. Figure 2 presents da/dN vs. f data for SA 304 SS tested in a pure H_2 gas environment at ambient temperature and reveals an additional HA-FCG response for SA 304 SS in high-pressure H_2. In the high f-regime, da/dN increased gradually with decreases in the test frequency, a similar response to the f-regime described by Eq. (4). In the intermediate f-regime, the EA-FCG attained a constant rate over an order of magnitude of the testing

frequency suggesting a saturation level for the effect of the environment has been attained. The onset of this regime was denoted as the critical frequency (f_{crit}) below which the EA-FCG rate would be f-independent. Further decreases in the frequency resulted in hydrogen degassing and consequently a sharp drop in the crack growth rate as can be seen in Fig. 2. The general trend of HA-FCG vs. frequency data for 304 SS in hydrogenated environments at room temperature can be summarized schematically in Fig. 3 which exhibits two ideal responses of EA-FCG rate over a wide range of applied frequencies. The f-dependent regime shows increased da/dN as the frequency decreases until a critical frequency is reached which marks the start of the second regime where the EA-FCG attains an upper bound rate (da/dN_{UB}), independent of the frequency below f_{crit}. In other words, the environmental effect reaches a saturation level at f_{crit} and can be quantified by the ratio of da/dN_{UB} to da/dN_{air}.
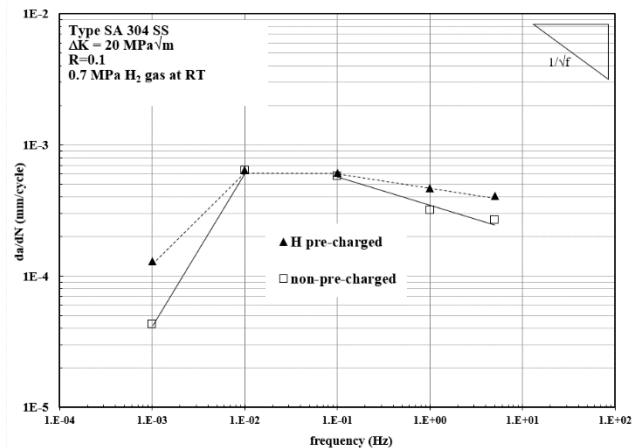

Fig. 2. FCG rate vs. loading frequency for SA 304 SS in pure hydrogen gas at room temperature. Data reproduced from [11].

Several research works have reported accelerated FCG of different ASS in LWRs environments compared to air at the same temperature with increased enhancement at a lower frequency and lower ΔK [1], [2], [3],[13]. Environmentally-assisted cracking in high-temperature water has been often ascribed to a slip-dissolution mechanism which suggests that the crack advances owing to localized metal dissolution after rupture of the passive film [14]. More recently, analysis of EA-FCG surfaces has revealed common similarities between ASS fracture surfaces produced in high-temperature water environments and specimens

charged with hydrogen before fatigue testing in air [15]. Furthermore, the characteristics of the deformed microstructure of an advancing fatigue crack-tip for ASS in high-temperature water have led many authors to suggest that H may play a major role in enhancing cracking by promoting slip planarity in high-temperature water environment [16], [15], [17].
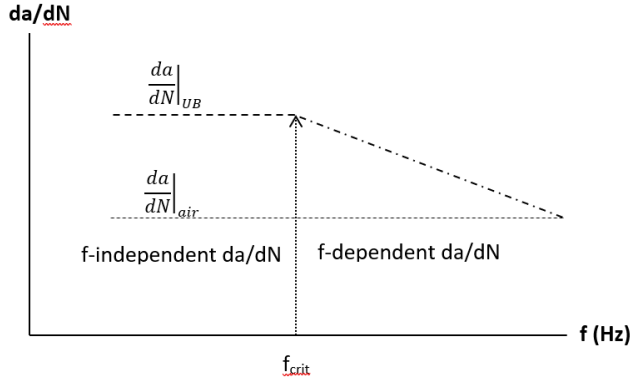

Fig. 3. A schematic diagram showing the hydrogen-assisted FCG rate vs. loading frequency for SA 304 SS in hydrogenated environments at room temperature.

IV. Proposed HA-FCG of 304 SS in BWR/HWC

Several crack tip processes have been identified that influence the HA-FCG in high-temperature water. Strain-induced α'-martensite phase transformation takes place in metastable 304 SS at ambient temperature [18]. However, at high-temperature LWR environments, austenite to martensite phase transformation is unlikely to happen since the operating temperature is higher than the temperature required to start the athermal transformation denoted as M_s. For a typical 304 SS composition in wt.% (0.06 C+18%Cr+0.85%Mn+8%Ni+0.45%Si), M_s can be estimated using Angel's relation [19]:

$$M_{d30}(°C) = 413 - 462 * (\%C + \%N) - 9.2 * (\%Si) - 8.1 * (\%Mn) - 13.7 * (\%Cr) - 9.5 * (\%Ni) - 18.5 * (\%Mo)$$

where M_{d30} is the temperature below which 50% of austenite transforms to martensite under the effect of a true deformation of 30%. The M_{d30} temperature for as-received 304 SS and 304L SS (%C=0.03) are calculated as 51.6 °C and 65.5°C, respectively. Therefore, fatigue cracks of 304/304L in BWR condition can be assumed to propagate through the austenitic phase. Second, H transport in austenite (face-centered cubic) is much slower than in the more

open crystal structure of ferrite (body-centered cubic) or martensite (body-centered tetragonal). The lattice hydrogen diffusion in austenitic 304 SS can be estimated using the following relation [20]:

$$D_\gamma = 2.01 x 10^{-6} \left(\frac{m^2}{s}\right) \exp\left(-\frac{47,000 \left(\frac{J}{mol}\right)}{RT}\right) (5)$$

applicable for 373 < T < 623 K. The diffusivity of H in austenite increases from $2.63x10^{-16}$ m²/s at room temperature [21] to $1.04x10^{-10}$ m²/s at 300°C, as predicted by Eq. (5). The high-temperature diffusivity is comparable to the room-temperature diffusivity of H in ferritic steel ($D_\alpha =1.55x10^{-10}$ m²/s) [22]. Thus, H diffusion in ASS in LWR environments is relatively rapid and may contribute to the f-dependent FCG behavior observed in Fig. 1. It should be noted that in BWRs, the high radiation field in the reactor core region causes radiolysis of the coolant steam and generates several oxidizing species such as O_2 and H_2O_2. H_2 is injected (1-2 ppm) to the coolant to remove such species giving rise to BWR/HWC environment [23]. BWR/HWC typically contains up to 10 ppb of H_2 [24]. Molecular hydrogen (H_2) can also be generated at the crack-tip by cathodic reactions accompanying the metal dissolution as described by Eq. (6):

$$H_2 + 2H_2O + 2e^- = 2OH^- + 2H_2 \qquad (6)$$
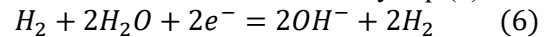
Hence, molecular hydrogen is abundant in BWR/HWC environments and may dissociate into atomic hydrogen at the crack tip and be absorbed into the metal according to Sievert's law.

V. Proposed HA-FCG Model

The frequency-dependent FCG of 304 SS in high-temperature water is assumed to be governed by H diffusion at the crack tip. The crack growth enhancement in the high-f regime is largely governed by the extent of diffusible H penetrating ahead of the crack tip, enhanced by the hydrostatic stress, and influenced by the distribution and nature of traps available along the cracking path [25]. Traps are less effective as the temperature is increased. The net result appears as an f-dependent FCG response described by Eq. (4). Owing to the lack of accurate modeling of the stress distributions in the process zone of a growing fatigue crack, the H and stress distributions for a given ΔK and frequency during the loading part of the fatigue cycle could be assumed to resemble the numerically predicted stress distributions ahead of a stationary crack at K_{max} available from the literature [26], [27],

[28]. Further, it is assumed that the time during the unloading cycle (K_{max} to K_{min}) has negligible contribution to H and crack-tip stress distributions for the succeeding loading cycle and hence the time available for H diffusion can be estimated as t = 1/(2f). The stress distributions for a stationary crack at K = K_{max} can be considered a reasonable approximation for a fatigue crack at the end of the loading cycle (K_{max} = ΔK/(1-R)), especially at low loading frequencies.

The proposed model is schematically shown in Fig. 4. It postulates that the HA-FCG rate per cycle at a given ΔK and frequency is controlled by the combined effects of the crack-tip tensile stress at K_{max} (mechanical effect) and the peak H lattice concentration (embrittlement effect). The critical frequency (f_{crit}) corresponds to the time required for H to reach, during a single loading cycle (~ 1/(2f_{crit})), the peak level at a distance (χ_{crit}) where the hydrostatic and local tensile stresses both are maximum. In other words, the largest crack extension per cycle occurs when the hydrogen lattice concentration C_L at χ_{crit} reaches its peak value at steady-state $C_{L,SS}$. This happens for all loading frequencies f $\leq f_{crit}$.
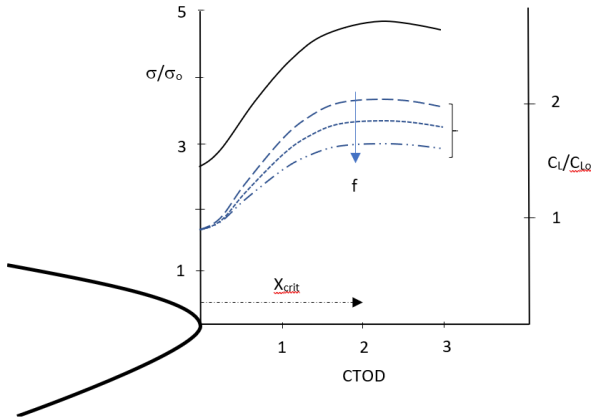

Fig. 4. *A schematic diagram for the proposed HA-FCG model showing the normalized tensile stress distribution (σ/σ_o) and the normalized hydrogen concentration profile (C_L/C_{Lo}) at the vicinity of a fatigue crack-tip at the end of a loading cycle for different frequencies.*

As the frequency is reduced, more time is available for H concentration to approach the steady-state H lattice concentration ($C_{L,SS}$). Therefore, an upper-bound f-independent HA-FCG rate can be predicted when both the local stress and the extent of embrittlement reach their maximum value ($C_L/C_{L,SS}$ = 1). Therefore, an upper-bound f-independent HA-FCG rate for f $\leq f_{crit}$ can be estimated as a first approximation to be equal to the distance ahead of the crack tip where the maximum local tensile stress coincides with the maximum hydrogen concentration:

$$\left.\frac{da}{dN}\right|_{UB} \approx \chi_{crit} \qquad (7)$$

For f > f_{crit}, da/dN is reduced in proportion to the reduction in the H concentration ratio. The predictive capability of the model depends on an accurate estimate of χ_{crit} (which represents the mechanical driving force for a fatigue crack growth event), and the normalized hydrogen concentration ($C_L/C_{L,SS}$)$^\varphi$ (which represents the simultaneous effects of H diffusion and trapping) [29].

Several FEM based analysis [26], [27], [28] have shown that the local tensile and hydrostatic stresses for a stationary crack are located at the same distance from the crack tip along the main crack plane and has been estimated in the order of twice the crack-tip opening displacement (CTOD). The CTOD for a stationary crack is given by:

$$\text{CTOD} \approx \beta \frac{K_{max}^2}{E'\sigma_o} \qquad (8)$$

where E' and σ_o is the elastic modulus (E'=E for plane stress and E/(1-v^2) for plane strain conditions) and the flow stress, respectively, and β is a proportionality constant. Therefore, the maximum HA-FCG at a given K_{max} can be estimated as:

$$\chi_{crit} \approx 2 * \text{CTOD} \qquad (9)$$

and hence,

$$\left.\frac{da}{dN}\right|_{UB} \approx 2 * \beta \frac{K_{max}^2}{E'\sigma_o} \qquad (10)$$

Owing to the lack of an analytical or numerical solution of the tensile and hydrostatic stress distributions ahead of a growing fatigue crack, Eq. (10) is employed to estimate the location of the maximum local tensile stress ahead of a growing fatigue crack based on the following assumptions. First, extending the stationary crack analysis to a fatigue crack could be considered as a first approximation for low-loading frequencies where FCG can be envisioned as quasi-static for each cracking event. Second, the general form of Eq. (10) is assumed to be applicable for high-temperature water such that encountered in LWRs environments by using temperature-dependent properties of E and σ_o. Third, small-scale yielding is assumed to prevail, and negligible creep-fatigue interaction at this homologous temperature (T_{Hom} =

T/T_m (K) = 573/1673 = 0.34). It should be pointed out that fracture surface analysis of laboratory samples suggests that creep has no significant contribution to FCG in BWR and PWR environments [30]. The following properties were obtained from the literature for 304 SS at a temperature around 300°C: E = 176 GPa [31], σ_o = 132 MPa [32], ν (Poisson's ratio) = 0.3 [33]. Thus, for 304 SS under constant amplitude fatigue loading in hydrogenated BWR environments, the upper-bound f-independent HA-FCG rate can be predicted by:

$$\left.\frac{da}{dN}\right|_{UB} \approx 78.3 x 10^{-9} * \beta * K_{max}^2 \qquad (11)$$

Eq. (11) represents the maximum f-independent HA-FCG rate for solution-annealed 304 SS for crack advancement controlled by H diffusion. The constant β can be estimated experimentally from EA-FCP data that exhibit f-independent behavior for $f < f_{crit}$. However, the author could not find f-independent HA-FCG data for 304 SS in high-temperature water to calibrate Eq. (11) for the constant β. For 304 SS in ambient water, β was estimated around 0.1 [29]. Figure 5 compares the predictions of the model using two values for β (0.1 and 0.3) with FCG rates for various 304 SS tested in BWR environments at the lowest frequencies reported in the literature. Several observations are highlighted regarding the model's prediction and limitations. First, the model predicts upper bound FCG rates for various 304 SS in different environments over a wide range of K_{max}.
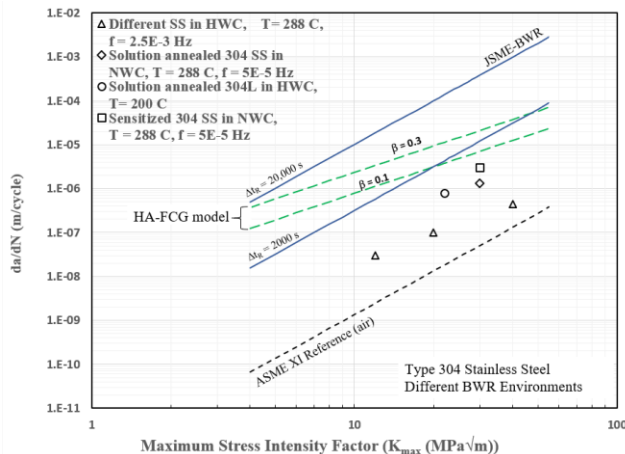

Fig. 5. Comparison of predictions of the HA-FCG model as a function of maximum applied stress intensity factor (K_{max}) with data for various 304 SS in BWR environments. Data from Reference [3]. JSME reference curves are plotted for BWR/NWC at $\Delta t_R = 2,000$ s and 20,000 s.

This is probably attributed to small variation in E and σ for SA 304 SS, sensitized 304 SS, and SA 304L. Second, the model shows a dependence on K_{max} raised to a power of 2 while the experimental data shows a slope of 2.4 [3]. More data are needed to verify the validity of the prediction model especially for FCG rates generated at $f << 10^{-5}$ Hz and da/dN vs. f data produced at a loading ratio higher than 0.1.

IV. Conclusions

EA-FCG of 304 SS in aqueous chloride solutions and in high-pressure H_2 at ambient temperature, and in high-temperature water exhibit an f-dependent response that can be described by a power law. A model is proposed based on hydrogen diffusion to predict an upper bound HA-FCG rate for 304 SS in BWR environments. The model predicts an upper-bound f-independent FCG rate as a function of mechanical loading parameters (ΔK and R) and the alloy tensile properties. The model predictions show a smaller margin of overestimation as compared to the current JSME reference code. Further verification with published data from the literature is underway especially for extremely low frequency and for higher R.

Acknowledgment

References

[1] T. Kawakubo, M. Hishida, K. Amano, M. Katsuta, Crack Growth Behavior of Type 304 Stainless steel in Oxygenated 290 °C Pure Water Under Low Frequency Cyclic Loading, Corrosion. 36 (1980) 638–647.

[2] G.L. Wire, W.J. Mills, Fatigue Crack Propagation Rates for Notched 304 Stainless Steel Specimens In Elevated Temperature Water , J. Press. Vessel Technol. 126 (2004) 318–326.

[3] H.P. Seifert, S. Ritter, H.J. Leber, Corrosion Fatigue Crack Growth Behaviour Of Austenitic Stainless Steels Under Light Water Reactor Conditions, Corros. Sci. 55 (2012) 61–75.

[4] M. Itatani, M. Asano, M. Kikuchi, S. Suzuki, Iida K., Fatigue Crack Growth Curve for Austenitic Stainless Steels in BWR

Environment, J. Press. Vessel Technol. 123 (2000)166–172.

[5] D.E. Allison, The Interaction Of Crack Geometry And Electrochemical Processes In Corrosion Fatigue Of AISI 304 Stainless Steel, Ph.D. Dissertation, Lehigh University, 1988.

[6] M. Gao, S. Chen, R.P. Wei, Crack Paths, Microstructure, And Fatigue Crack Growth In Annealed And Cold-Rolled AISI 304 Stainless Steels, Metall. Trans. A. 23 (1992) 355–371.

[7] S.-F. Chen, Corrosion Fatigue Crack Growth and Electrochemical reactions in an Annealed Fe-18Cr-12Ni Alloy, M.S. Thesis, Lehigh University, 1992.

[8] B.M. Al-Jarallah, Frequency Effect on Corrosion Fatigue Crack Propagation of Different Microstructures of AISI 304 Type Stainless Steel, M.S. Thesis, King Fahd University pf Petroleum and Minerals, 2007.

[9] Z.M. Gasem, B.M. Al-Jarallah, Effect of Sensitization on Corrosion Fatigue Crack Propagation of Type 304 Stainless Steel in 3.5% NaCl, in: NACE - Int. Corros. Conf. Ser., 2012: pp. 4885–4890.

[10] H. Matsunaga, T. Nakashima, K. Yamada, T. Matsuo, J. Yamabe, S. Matsuoka, Effect Of Test Frequency On Hydrogen-Enhanced Fatigue Crack Growth In Type 304 Stainless Steel And Ductile Cast Iron, in: PVP2016, ASME, 2016: pp. 1–5.

[11] H. Matsunaga, O. Takakuwa, J. Yamabe, S. Matsuoka, Hydrogen-Enhanced Fatigue Crack Growth In Steels And Its Frequency Dependence, Philos. Trans. R. Soc. A Math. Phys. Eng. Sci. 375 (2017).

[12] Y. Ogawa, S. Okazaki, O. Takakuwa, H. Matsunaga, The Roles Of Internal And External Hydrogen In The Deformation And Fracture Processes At The Fatigue Crack Tip Zone Of Metastable Austenitic Stainless Steels, Scr. Mater. 157 (2018) 95–99.

[13] M.F. Chiang, M.C. Young, J.Y. Huang, Effects Of Hydrogen Water Chemistry On Corrosion Fatigue Behavior Of Cold-Worked 304L Stainless Steel In Simulated BWR Coolant Environments, J. Nucl. Mater. 411 (2011) 83–89.

[14] P.L. Andresen, F. Peter Ford, Life Prediction By Mechanistic Modeling And System Monitoring Of Environmental Cracking Of Iron And Nickel Alloys In Aqueous Systems, Mater. Sci. Eng. A.

103 (1988) 167–184.

[15] K. Mukahiwa, F. Scenini, M.G. Burke, N. Platts, D.R. Tice, J.W. Stairmand, Corrosion Fatigue And Microstructural Characterisation Of Type 316 Austenitic Stainless Steels Tested In PWR Primary Water, Corros. Sci. 131 (2018) 57–70.

[16] G.L. Wire, W.J. Mills, Fatigue Crack Propagation Rates For Notched 304 Stainless Steel Specimens In Elevated Temperature Water, J. Press. Vessel Technol. Trans. ASME. 126 (2004) 318–326.

[17] B.D. Miller, T.W. Webb, Understanding The Effect Of Crack Tip Deformation On Fatigue Crack Growth Behavior In 300-Series Austenitic Stainless Steel, Int. J. Fatigue. 125 (2019) 261–270.

[18] G. Schuster, C. Altstetter, Fatigue Of Annealed And Cold Worked Stable And Unstable Stainless Steels, Metall. Trans. A. 14 (1983) 2077–2084.

[19] Y. Mine, C. Narazaki, K. Murakami, S. Matsuoka, Y. Murakami, Hydrogen Transport in Solution-Treated And Pre-Strained Austenitic Stainless Steels And Its Role in Hydrogen-Enhanced Fatigue Crack Growth, Int. J. Hydrogen Energy, 34 (2009) 1097–1107.

[20] C.S. Marchi, B.P. Somerday, S.L. Robinson, Permeability, Solubility And Diffusivity Of Hydrogen Isotopes In Stainless Steels At High Gas Pressures, Int. J. Hydrogen Energy. 32 (2007) 100–116.

[21] Y. Mine, Z. Horita, Y. Murakami, Effect Of Hydrogen On Martensite Formation In Austenitic Stainless Steels in High-Pressure Torsion, Acta Mater. 57 (2009) 2993–3002.

[22] H.G. Nelson, Hydrogen Embrittlement, Treatise Mater. Sci. Technol. 25 (1983) 275–359.

[23] D. Tice, Contribution Of Research To The Understanding And Mitigation Of Environmentally-Assisted Cracking In Structural Components In Light Water Reactors, Eur. Corros. Congr. EUROCORR 2016. 3 (2016) 1953–1973.

[24] S. Mohanty, S. Majumdar, K. Natesan, A Review of Stress Corrosion Cracking / Fatigue Modeling for Light Water Reactor Cooling System Components Nuclear Engineering Division Argonne National Laboratory, Nucl. Energy. (2012).

[25] A. Turnbull, Perspectives On Hydrogen Uptake, Diffusion And Trapping, Int. J. Hydrogen Energy. 40 (2015) 16961–16970.

[26] P. Sofronis, R.M. McMeeking, Numerical Analysis Of Hydrogen Transport Near A Blunting Crack Tip, J. Mech. Phys. Solids. 37 (1989) 317–350.

[27] A.H.M. Krom, R.W.J. Koers, A. Bakker, Hydrogen Transport Near A Blunting Crack Tip, J. Mech. Phys. Solids. 47 (1999) 860–881.

[28] C. V. Di Leo, L. Anand, Hydrogen In Metals: A Coupled Theory For Species Diffusion And Large Elastic-Plastic Deformations, Int. J. Plast. 43 (2013) 42–69.

[29] Z.M. Gasem, Modeling Frequency-Dependent Hydrogen-Assisted Fatigue Crack Growth in Type 304 Stainless Steel in Ambient Condition, to be submitt. to Eng. Fract. Mech. (2023).

[30] S.L. Medway, D.R. Tice, N. Platts, A. Griffiths, G. Ilevbare, R. Pathania, Mechanistic Understanding Of Environmentally Assisted Fatigue Crack Growth Of Austenitic Stainless Steels In PWR Environments, in: Miner. Met. Mater. Ser., 2018: pp. 957–986.

[31] R.M. Digilov, Flexural Vibration Test Of A Cantilever Beam With A Force Sensor: Fast Determination Of Young's Modulus, Eur. J. Phys. 29 (2008) 589–597.

[32] L. Yu, R.G. Ballinger, X. Huang, M.M. Morra, L.B. O'Brien, D.J. Paraventi, V.S. Smentkowski, P.W. Stahle, Corrosion Fatigue Behavior Of Austenitic Stainless Steel in a Pure D_2O Environment, in: Miner. Met. Mater. Ser., 2018: pp. 943–956.

[33] INCO, Austenitic Chromium-Nickel Stainless Steels — Engineering Properties At Elevated Temperatures, 2021.